Physica C 484 (2013) 52–55

Contents lists available at SciVerse ScienceDirect

Physica C

journal homepage: www.elsevier.com/locate/physc

Tunneling break-junction measurements of the superconducting gap in Y_2C_3

T. Ekino [a,*], A. Sugimoto [a], A.M. Gabovich [b], H. Kinoshita [c], J. Akimitsu [c]

[a] Hiroshima University, Graduate School of Integrated Arts and Sciences, Higashi-Hiroshima 739-8521, Japan
[b] Institute of Physics, National Academy of Sciences of Ukraine, Kyiv 03680, Ukraine
[c] Aoyama-Gakuin University, Department of Physics and Mathematics, Sagamihara 229-8558, Japan

ARTICLE INFO

Article history:
Accepted 19 March 2012
Available online 28 March 2012

Keywords:
Y_2C_3
Superconducting energy gap
Tunneling
Break junction

ABSTRACT

Tunneling measurements of the electron spectrum in the superconducting state have been carried out in Y_2C_3 samples with the bulk (resistive and diamagnetic) critical temperature $T_c = 15$–16 K. A break-junction technique was crucial to find the intrinsic gap features. The representative gap structure at 4 K reveals distinct BCS-like peaks with the gap value of $2\Delta(4\text{ K}) = 3$–4 meV. Assuming local T_c values of 10–13 K, the characteristic gap to T_c ratio $2\Delta/k_BT_c$ (k_B is the Boltzmann constant) was found to possess the BCS weak-coupling value 3.5 ± 0.2, appropriate to isotropic *s*-wave superconductors.

1. Introduction

A cubic Pu_2C_3-type sesquicarbide compound Y_2C_3 is a non-centrosymmetric superconductor showing a critical temperature T_c approximately equal to 18 K, which is a relatively high T_c among intermetallic superconductors [1]. Since the crystal inversion center does not exist in this compound, which might be a smoking gun of an unconventional superconductivity [2,3], it is worth to study superconducting properties of Y_2C_3 in terms of the order parameter symmetry as well as an underlying pairing mechanism.

We note that specific-heat measurements clarified that the temperature, T, dependence of the specific-heat electronic component exhibits a simple exponential dependence below T_c. It testifies that superconductivity is most probably an isotropic, *s*-wave one [4]. On the contrary, the observed magnetic field dependence of the electronic specific heat contradicts the scenario of the conventional superconductivity. Indeed, recent NMR and penetration depth measurements suggested that Y_2C_3 reveals spin–singlet, two-gap features with the gap values of $2\Delta(0) = 5\ k_BT_c$ and (1–2) k_BT_c [5–7]. Moreover, the T-dependence of the spin–lattice relaxation rate deviates from the *s*-wave Bardeen–Cooper–Schrieffer (BCS) behavior, and the penetration depth exhibits a linear T-dependence at low T, which corresponds to the non-conventional order parameter symmetry [7]. Such ambiguities might be a consequence of the microscopic inhomogeneities inherent to the compound concerned, so that the observed T-dependences result from a spatial averaging, vary among different samples and manifest themselves differently for various measured quantities [8]. Therefore, local more or less not averaged probes are highly desirable to elucidate peculiarities of the intrinsic energy gap distribution.

In this paper we present the electron-tunneling measurements of the superconducting gaps in Y_2C_3. Electron-tunneling spectroscopy provides an essential method to determine the superconducting gap structure by directly measuring electron currents across junctions, so that the electron spectrum in the superconducting state is probed by charge carriers themselves. The tunnel conductance, $G(V) = dI/dV\,(V)$, derived from current (I)–voltage (V) characteristics of the break junction is directly proportional to the convolution of the quasiparticle densities of states from both pieces of the broken superconductor, thus giving a significant information about the gap structure.

2. Experimental procedure

Since Y_2C_3 is chemically very reactive and unstable in the open air, its tunnel spectra have not been measured until now. We applied here the break-junction technique [9,10] to find the intrinsic gap features in this delicate material. A crucial advantage of this technique is a cryogenic (4 K) fracturing of the sample piece fixed with four electrodes by applying an external bending force, resulting in a fresh and clean junction interface. This junction design forms predominantly superconductor–insulator–superconductor (SIS) junctions. Polycrystalline samples were prepared by arc melting, followed by high-pressure (4–5.5 GPa) and high-temperature (1673–1873 K) treatments to produce a sesquicarbide phase. Powder X-ray diffraction showed that each sample is a single-phase one.

3. Results and discussion

The T dependence of resistivity is displayed in Fig. 1. The onset $T_c \approx 15.9$ K is in a good agreement with that demonstrated by susceptibility measurements. The latter are shown in the inset of

* Corresponding author. Tel.: +81 82 424 6552; fax: +81 82 424 0757.
E-mail address: ekino@hiroshima-u.ac.jp (T. Ekino).

0921-4534/$ - see front matter © 2012 Elsevier B.V. All rights reserved.
http://dx.doi.org/10.1016/j.physc.2012.03.044

Fig. 1. The zero-resistance critical temperature is observed to be 15.4 K. It is smaller than the onset one and reveals a sharp resistive transition of the width $\Delta T = 0.5$ K. The true zero resistance displayed in Fig. 1 was observed for the first time only after Au spots were put on the sample surface as current and potential electrodes. We note that Au conducting paste directly attached to the sample surface caused substantial residual resistance below T_c, which indicates seriously reactive surface nature of Y_2C_3.

Fig. 2 shows representative conductances $G(V)$ obtained for different break junctions at about 4 K. The distinct gap-edge conductance peaks are clearly visible in Fig. 2a with the bias-voltage peak-to-peak distance $V_{p-p} = 6$ mV. The sub-gap structure in Fig. 2a may be due to a direct current passing through a weak-link constriction or to multiple Andreev-reflection harmonics [11]. The curve Fig. 2b is asymmetric with respect to the bias voltage, reflecting the tunneling barrier asymmetry of the break junction arising from the crack occurring close to the grain boundary of the sample, as is discussed later.

To analyze these conductance features, the fitting procedures were employed using the broadened BCS density of states,

$$D(E,\Gamma) = \mathrm{Re}\left\{\frac{E - i\Gamma}{\sqrt{(E - i\Gamma)^2 - \Delta^2}}\right\}, \quad (1)$$

which takes into account the quasiparticle energy smearing [12]. Here, Γ represents a phenomenological broadening parameter of whatever origin. For Fig. 2a, the SIS conductance was suggested, while for the broader gap structure of Fig. 2b the calculation was done assuming a superconductor–insulator–normal metal (SIN) junction to occur. The correspondence between the experimental and the calculated curves is satisfactory as shown in Fig. 2. Thus, the superconducting gap in Y_2C_3 is found to possess the isotropic *s*-wave symmetry of the order parameter.

The SIN junction type revealed in Fig. 2b is most probably caused by the break coincidence with the grain boundary, where one of the electrodes is in a normal-metal state. The gap magnitudes were $2\Delta(T) = 3.0$–4.2 meV with $\Gamma = 0.09$–0.27 meV. Since the relative broadenings $\Gamma/\Delta \sim 0.06$–0.13 obtained here are of the same order of magnitude as that found in our previous break-junction measurements of various BCS superconductors, Γ is most probably due to some more or less trivial effects associated with interface properties [10,13]. The gap value $2\Delta = 3.0$ meV of Fig. 2a is exactly in accord with $V_{p-p} = 6$ mV for the SIS junction because V_{p-p} should be equal to $4\Delta/e$, where e is the (positive) elementary charge. On the other hand, $2\Delta = 4.2$ meV for the SIN junction in Fig. 2b corresponds to $\approx 0.6\ V_{p-p}$, because the value of V_{p-p} is ≈ 7 mV. This discrepancy might be due to the fact that the piling up of the convoluted singularities appropriate to the BCS densities of states occurs only in the SIS junctions and survives averaging over microscopic inhomogeneities [14,15] simulated by Γ in our fitting. On the contrary, conductance of the SIN junction, which is determined by a single BCS density of states, is not so steep and is more effectively smeared by Γ.

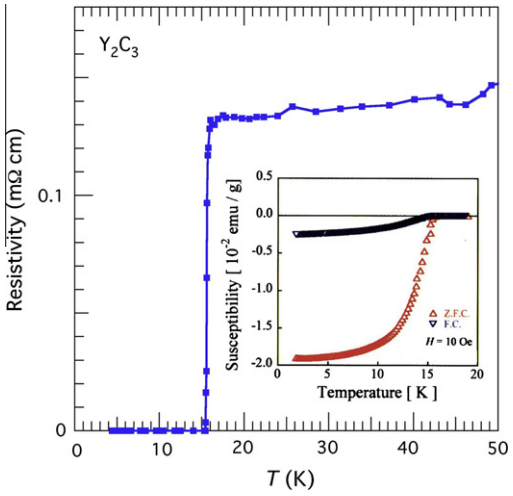

Fig. 1. Temperature, T, dependence of the resistivity for Y_2C_3. Inset shows the diamagnetic susceptibility as a function of T.

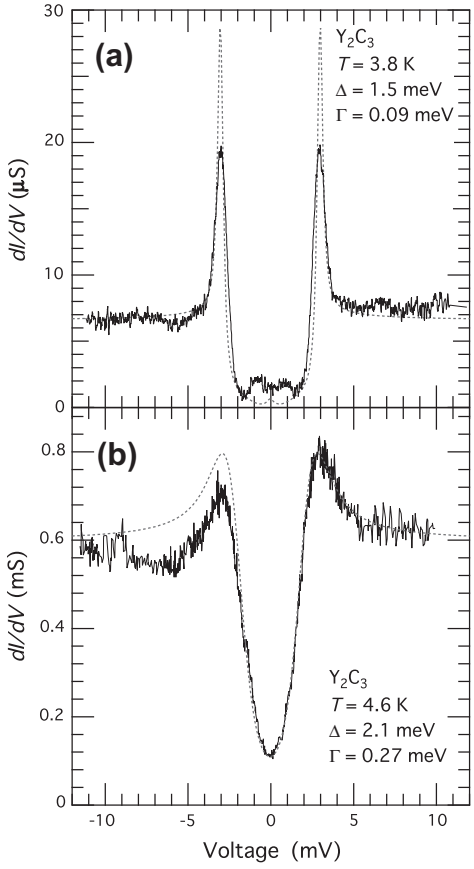

Fig. 2. Tunneling conductance $G(V)$ for different Y_2C_3 break junctions. The dotted curves were calculated using Eq. (1).

In this connection, the V_{p-p} of the SIS junction is always equal to $4\Delta/e$ regardless of the tunneling barrier quality as is shown in Fig. 3. The evidence of the SIS junction formation can be readily seen, because noticeable quasiparticle peaks as well as zero-bias signatures of the Josephson currents are observed. As is unambiguously observed in Fig. 3, the bias positions of the conductance peaks do not conspicuously shift when the broadening of the spectra and the leakage effects differ substantially due to varying external bending forces. The variations of the latter lead to different interface electron properties of the junction area [13]. Therefore, in order to properly examine the gap structure and, in particular, the symmetry of the superconducting order parameter by the tunneling spectroscopy, high-quality junctions should be prepared and measured.

The results found for both SIS and SIN junctions are consistent, clearly indicating that superconducting Y_2C_3 samples have a conventional BCS density of states. This is in contrast to the previous reports of the multiple-gap and/or nodal-gap structures, appropriate to the material concerned [5–7]. The apparent discrepancy can be explained as follows. All conclusions supporting non-conventional complex nature of superconductivity in Y_2C_3

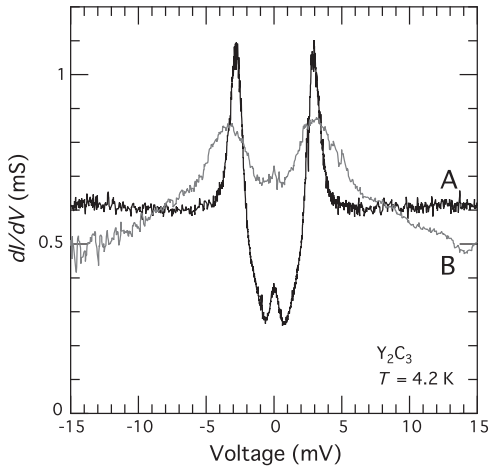

Fig. 3. $G(V)$ for Y_2C_3 measured for a break junction. Curves A and B represent measurements with different external bending forces and, as a consequence, varying interface conditions.

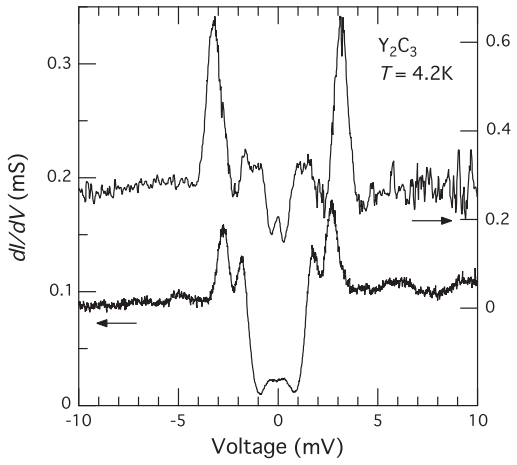

Fig. 4. $G(V)$ for roughly treated Y_2C_3 samples showing multiple gap structures. Curves A and B correspond to different break junctions.

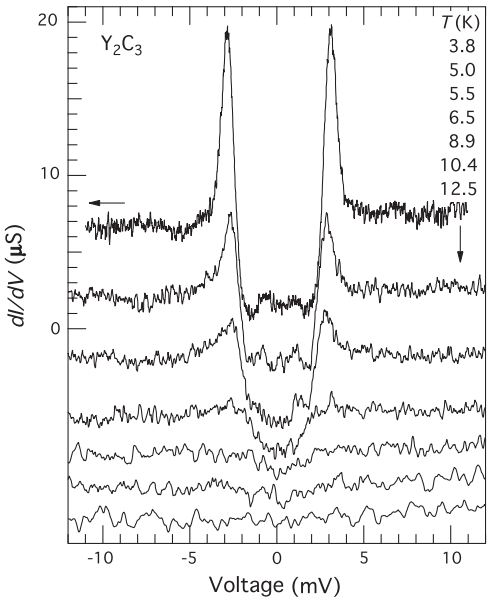

Fig. 5. T-evolution of $G(V)$ for Y_2C_3. The junction is the same as that of Fig. 2a.

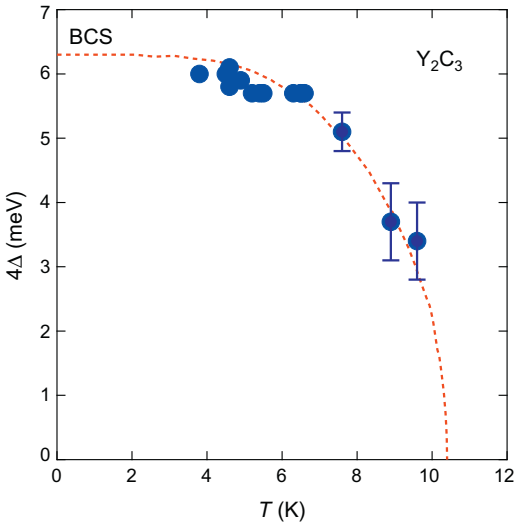

Fig. 6. T-dependence of the peak position $eV_{p-p} = 4\Delta(T)$ for $G(V)$ presented in Fig. 5. The broken line represents the BCS prediction.

were made on the basis of studied temperature dependences of *integrated* physical quantities, describing averaged and distorted electron properties of unstable samples. Hence, intrinsic microscopic features were hidden. Since the Y_2C_3 compound is extraordinary sensitive to air humidity and mechanical damage, peculiar phase separations and nanoscale inhomogeneities appear under usual treatment conditions. Indeed, our reference measurements using roughly treated (long-term air exposed) samples exhibit apparent multi-gap structures and/or high offsets of the zero-bias conductance, as is shown in Fig. 4. The results therefore indicate that the degradation by exposing to the air easily penetrates into the deeply inside of the solid sample. Nevertheless, the gap structure is clearly seen even under those rugged circumstances.

Fig. 5 shows the temperature evolution of $G(V)$. The lowest-T data are the same as shown in Fig. 2a. In Fig. 5, the distinct gap-edge peaks clearly seen at $T = 3.8$ K as well as the distance between them are gradually suppressed and shrunk, respectively, when T increases, and eventually $G(V)$ flattens at around 10 K. This feature is quite common to SIS junctions made of conventional BCS superconductors [10,12,13]. The traces of the gap disappear at much lower temperatures than the nominal bulk $T_c = 15$–16 K seen in Fig. 1. Those reduced temperatures can be regarded as local critical temperatures for specific junctions, varying due to the microscopic inhomogeneity of the samples, caused by peculiarities of the synthesis process. At the same time, gap features appropriate to $G(V)$ of the SIN junction and depicted in Fig. 2b simply broaden upon warming and disappear at about 13 K, as is usually seen for the BCS superconductors.

The temperature dependence of the gap value from Fig. 5 is plotted in Fig. 6, which is obtained by tracking the peak position of $G(V)$ as a function of temperature. This is justified because peaks in $G(V)$ for a SIS junction directly measure the gap-related value $4\Delta(T)$ up to near T_c [10,13]. As is shown in Fig. 6, the behavior of $\Delta(T)$ reasonably agrees with the BCS prediction, from which T_c is determined to be 10.4 K. We note that such local T_c values, being substantially lower than the bulk $T_c = 16$ K, are often observed as shoulders in the T-dependent susceptibility for the samples synthesized under non-optimal conditions. Similar Y_2C_3 samples with lower bulk T_c values were examined in detail and were

demonstrated to have slightly larger (~0.5%) lattice parameters as compared with those of the optimally synthesized samples [1]. Such a unique behavior may be caused by a variation of the C content under different heat-treatment conditions. This instability, in its turn, demonstrates the importance of the light C atom and its optical vibrations as a source of superconductivity in Y_2C_3.

In our measurements, the characteristic gap to T_c ratio $2\Delta(0)/k_BT_c$ is observed to be 3.4–3.7, which is in a fairly good agreement with the weak-coupling value 3.52 appropriate to *s*-wave BCS superconductors. Break-junction data presented here indicate that the gap to T_c ratio $2\Delta(0)/k_BT_c$ badly correlates with the local T_c. Namely, it varies from 3.4 up to 3.7 for T_c in the range 10–13 K. The revealed single isotropic *s*-wave gap pattern with $\Delta(0)$ depending on T_c is consistent with the results of the specific-heat measurements. However, the latter exhibit the strong-coupling-like gap to T_c ratio $2\Delta(0)/k_BT_c$ up to 5.4 for $T_c \approx 15$ K [4].

4. Conclusion

Tunneling measurements of the sesquicarbide superconductor Y_2C_3 with the bulk T_c = 15–16 K have been carried out for the first time. The break-junction technique was helpful to reveal the intrinsic electronic properties by avoiding chemical reactions of this unstable compound during measurements. The results showed the conventional *s*-wave BCS gap structure. The superconducting gap magnitudes $2\Delta(4\text{ K}) = 3.0$–$4.2$ meV lead to the gap to T_c ratios $2\Delta(0)/k_BT_c = 3.3$–3.7, taking into account the local T_c being 10–13 K. Thus, superconductivity in Y_2C_3 is, most probably, the weak coupling, isotropic one. It would be highly desirable to investigate Y_2C_3 samples with the highest local T_c = 18 K to find the upper limit for the characteristic gap to T_c ratio in this compound.

Acknowledgements

We would thank the Natural Science Center for Basic Research and Development, Hiroshima University for supplying liquid helium and the EPMA element analysis. This research was supported by Grant-in-Aid for Scientific Research (No. 19540370) from JSPS, Japan. AMG is indebted to the 2010 Visitors Program of the Max Planck Institute for the Physics of Complex Systems (Dresden, Germany) as well as the Project No. 8 of the 2012–2014 Scientific Cooperation Agreement between Poland and Ukraine.

References

[1] G. Amano, S. Akutagawa, T. Muranaka, Y. Zenitani, J. Akimitsu, J. Phys. Soc. Jpn. 73 (2004) 530.
[2] L.P. Gor'kov, E.I. Rashba, Phys. Rev. Lett. 87 (2001) 037004.
[3] S. Fujimoto, J. Phys. Soc. Jpn. 76 (2007) 051008.
[4] S. Akutagawa, J. Akimitsu, J. Phys. Soc. Jpn. 76 (2007) 024713.
[5] H. Harada, S. Akutagawa, Y. Miyamichi, H. Mukuda, Y. Kitaoka, J. Akimitsu, J. Phys. Soc. Jpn. 76 (2007) 023704.
[6] S. Kuroiwa, Y. Saura, J. Akimitsu, M. Hiraishi, M. Miyazaki, K.H. Satoh, S. Takeshita, R. Kadono, Phys. Rev. Lett. 100 (2008) 097002.
[7] J. Chen, M.B. Salamon, S. Akutagawa, J. Akimitsu, J. Singleton, J.L. Zhang, L. Jiao, H.Q. Yuan, Phys. Rev. B 83 (2011) 144529.
[8] T. Ekino, A.M. Gabovich, T. Takasaki, A.I. Voitenko, J. Akimitsu, H. Fujii, T. Muranaka, Physica C 426–431 (2005) 230–233.
[9] T. Ekino, T. Takabatake, H. Tanaka, H. Fujii, Phys. Rev. Lett. 75 (1995) 4262.
[10] T. Ekino, H. Fujii, T. Nakama, R. Yagasaki, Phys. Rev. B 56 (1997) 7851.
[11] J. Lantz, V.S. Shumeiko, E. Bratus, G. Wendin, Phys. Rev. B 65 (2002) 134523.
[12] R.C. Dynes, V. Narayanamurti, J.P. Garno, Phys. Rev. Lett. 41 (1978) 1509.
[13] T. Ekino, H. Fujii, M. Kosugi, Y. Zenitani, J. Akimitsu, Phys. Rev. B 53 (1996) 5640.
[14] T. Ekino, A.M. Gabovich, A.I. Voitenko, Fiz. Nizk, Temp. 34 (2008) 515 (Low Temp. Phys. 34 (2008) 409).
[15] T. Ekino, A.M. Gabovich, Mai Suan Li, M. Pękała, H. Szymczak, A.I. Voitenko, J. Phys. Condens. Matter 20 (2008) 425218.